Mon. Not. R. Astron. Soc. **305,** L55–L58 (1999)

The *Hubble Deep Field* North reveals a supernova at $z \sim 0.95$

F. Mannucci[1] and A. Ferrara[2,3]
[1]*CAISMI–CNR, Largo E. Fermi 5, 50125 Firenze, Italy*
[2]*Osservatorio Astrofisico di Arcetri, Largo E. Fermi 5, 50125 Firenze, Italy*
[3]*Joint Institute for Laboratory Astrophysics, University of Colorado, Boulder, CO 80309, USA*

Accepted 1999 March 22. Received 1999 March 22; in original form 1999 January 27

ABSTRACT

We report the discovery of a variable object in the *Hubble Deep Field* North (HDF-N) which brightened, during the 8.5 d sampled by the data, by more than 0.9 mag in I_{814} and about 0.7 mag in V_{606}, remaining stable in B_{450}. Subsequent observations of the HDF-N show that two years later this object has dimmed to about its original brightness in I_{814}. The colours of this object, its brightness, its time behaviour in the various filters and the evolution of its morphology are consistent with it being a Type Ib supernova in a faint galaxy at $z \sim 0.95$.

Key words: supernovae: general – cosmology: observations – early Universe.

1 INTRODUCTION

The discovery of supernovae (SNe) in the early Universe is of great interest because they can provide a wealth of information about cosmological parameters and the cosmic star formation history. It is now believed that the star formation activity in the Universe probably started in small objects which later on merged to form larger units (Couchman et al. 1986; Ciardi et al. 1997; Haiman, Rees & Loeb 1997; Tegmark et al. 1997; Ferrara 1998). Unless the initial mass function (IMF) at high z is drastically different from the local one, some of the stars formed will end their lives as SNe. Detecting high-z SNe would be of primary importance to clarify how reionization and rehating of the Universe proceeded (Ciardi et al. 1997), and, in general, to derive the star formation history of the Universe (Sadat et al. 1998; Madau, Della Valle & Panagia 1998) and put constraints on the IMF and chemical enrichment of the Universe.

Great effort has been put into this search (Garnavich et al. 1998; Perlmutter et al. 1998), and many SNe have been found up to a redshift of $z = 1.20$ (Aldering 1998) when the Universe was only about half of its present age. The HDF images (Williams et al. 1996) are the among the deepest taken to date and in principle could contain SNe up to $z \sim 3$. Two SNe were actually detected by Gilliland & Phillips (1998) by comparing the primary HDF-N data with second-epoch images taken two years later. The primary observations of this field were taken using four optical filters centred at 3000 Å (U_{300}), 4500 Å (B_{450}), 6060 Å (V_{606}) and 8140 Å (I_{814}) during a time span of about 10 d in 1995 December. Although the distribution of the data over this period is not uniform, the overall time coverage is good enough to detect objects with significant variations on time-scales of a few days. High-redshift SNe cannot be identified near their maximum in such a short time span because they vary too slowly, but soon after the explosion they evolve fast enough to be detected.

How many SNe can be expected in the HDF-N? This number can be estimated using the computations by Marri & Ferrara (1998) and Marri, Ferrara & Pozzetti (1998) for future *Next Generation Space Telescope* (*NGST*) surveys. Scaling their results for a flat cold dark matter (CDM) + Λ universe with $\Omega_{\rm M} = 0.4$ to the HDF-N area ($\sim$5 arcmin^2) and assuming a surveying time of $\sim$8 d (see below), we obtain an expected number $\sim$0.34 SNe from massive stars (SN Types Ib/II). As a comparison, scaling the analytical estimates of Miralda-Escudé & Rees (1997) to the HDF-N, one obtains a similar expected rate of 0.17 SNe in the HDF-N. These values are large enough to encourage a new analysis of the HDF-N.

2 OBJECT SELECTION, PHOTOMETRY AND MORPHOLOGY

The original observations of the HDF-N in each filter consisted of about 300 images taken in several (from 9 to 11, depending on the filter) positions on the sky (dither positions). We have divided these images into a few consecutive groups, three for V_{606} and I_{814} and two for B_{450}. The U_{300} band, which is intrinsically less efficient, was not considered. The HDF-N was observed again two years later in U_{300} and I_{814} and the latter image (*I*4 in Table 1) is deep enough to be used for this project.

Where possible, images taken in the same position on the sky were not split into different groups so that we could make effective use of those combined by the HDF working team (Williams et al. 1996) for each dither position, and made available on the Web. Some dither positions in V_{606} and I_{814} contain images too widely separated in time, and therefore have been split. In this case the frames were reduced by the automatic pipeline provided by the ST-ECF Web site. In all cases warm and bad pixels were rejected using the standard routines.

Given the small number of images, between three and six, present in some of the final groups, it was not possible to use the

Table 1. Grouping of the images and properties of 2-584.2.

Filter	Image	Dither position[a]	Exp. time (hours)	Time range (days)	Limit[b]	2-584.2 Mag.	2-584.2 SNR[c]
F450W	Total		33.5	0.00–9.21	29.72	28.73	5.1
	*B*1	6A + 9 + 4 + 5 + 3 + 8 + 1 + 2	28.2	0.00–3.15	29.64	28.75	7.5
	*B*2	7 + 6B	5.3	8.34–9.21	28.72	28.41	3.8
F606W	Total		30.3	1.48–10.07	30.07	28.78	7.2
	*V*1	3 + 2 + 6A + 4A	5.6	1.48–5.56	29.16	29.14	3.1
	*V*2	9A + 5A + 7 + 1 + 11 + 10	14.7	6.43–8.51	29.68	28.93	6.0
	*V*3	8 + 6B + 4B + 9B + 5B	10.0	8.57–10.07	29.47	28.53	7.2
F814W	Total		34.3	3.21–10.10	29.46	28.63	4.8
	*I*1	2 + 1 + 6	10.0	3.21–4.35	28.80	>28.80	2.8
	*I*2	4A + 9 + 3 + 5A	14.5	4.69–6.30	29.00	28.76	3.8
	*I*3	8 + 7 + 11 + 4B + 5B	9.8	6.63–10.10	28.79	28.05	6.0
	*I*4		15.6	735–738	29.00	>29.00	2.9

[a] Dither positions as in Williams et al. (1996). When present, A and B refer to the first and second parts of the split positions.
[b] 3σ limit for point sources.
[c] Signal-to-noise ratio of the photometry.

'drizzle' algorithm (Fruchter et al. 1997) often used for the Wide Field Planetary Camera (WFPC2) data reduction. We have chosen to resample all the images to a pixel of 0.05 arcsec (half of the original WF pixel scale) and use the IRAF task IMCOMBINE to make the final combinations while rejecting deviant pixels. This procedure is more efficient than drizzle in rejecting any residual warm and bad pixels; this is especially true for the final V_{606} and I_{814} images which contain five dither images each. Table 1 lists the properties of the resulting images, with their time coverage and limiting magnitude.

Two tests were performed to check the data reduction results. (i) The fluxes of a few compact sources from the list of Méndez et al. (1996) were measured in each of the resulting images to verify the constancy of the photometry. (ii) As discussed, for example, by Ferguson (1998), the effective limiting magnitude depends on the object size as much as on its total magnitude. The detection limits for point sources in the images were measured by adding stars and detecting them using FOCAS (Valdes 1982); the derived values for the 80 per cent completeness level are in good agreement (within 0.1 mag) with the values of Williams et al. (1996) once their 10σ limits in an aperture of 0.5 arcsec diameter are scaled for the exposure time and to about 3σ in a 0.30 arcsec diameter aperture, which yields the highest signal-to-noise ratio for point source photometry (e.g. Thompson 1995). These values are listed in Table 1; all magnitudes are in the *AB* system.

The three combined V_{606} images (V1, V2 and V3), showing the best sensitivity (3σ limits between 29.1 and 29.7) and time coverage (about 8.5 d), were examined for variable objects having a monotonic trend, either brightening or dimming. A few interesting objects were selected; the most remarkable one is in chip 2 of the WF camera and is present in the Williams et al. (1996) catalogue with the entry number 584.2. The J2000 coordinates of this object (2-584.2) are $12^{\rm h}36^{\rm m}49\overset{\rm s}{.}357$, $+62°14'37\overset{''}{.}50$. In the total images, this object has flat B_{450}, V_{606} and I_{814} colours and is undetected in U_{300}; however, it cannot be classified as a U_{300} drop-out, being too faint to show a strong enough break between U_{300} and B_{450}.

Table 1 and Fig. 1 show the time evolution of the photometry of 2-584.2. Its magnitudes in the various images were measured inside a circular aperture of 0.3 arcsec, corresponding to about twice the point spread function FWHM, and corrected to an infinite aperture. This object shows a strong brightening in both V_{606} and I_{814}, while the photometry in the B_{450} band is consistent with a constant value. The errors shown in Fig. 1 are derived under the assumption of Poisson noise inside the photometric aperture.

We have computed the statistical significance of the detected variation. For the V_{606} band we consider the two differences $V2 - V1$ and $V3 - V2$; in the I_{814} band, as the object shows no significant variation among *I*1, *I*2 and *I*4, we co-add these three images and compare the result with *I*3. By comparing the differences in the photometry with the quadratic sum of the errors, we find a joint probability for these three variations to arise from noise of 1.2×10^{-5}. In the HDF-N there are about 1200 objects between $I_{814} = 27$ and 29 (Williams et al. 1996), therefore we expect one such spurious event only every 70 HDFs.

Fig. 2 shows the images of this object in the various bands[1] in the total images the object is marginally resolved in B_{450} and V_{606}, whereas in I_{814} it is consistent with a point source. The images also give the impression of a 'sharpening' of 2-584.2 with time: the object seems more extended at the beginning of the observations than at the end, as if a bright core were emerging in V_{606} and I_{814}. Its faintness prevents us from studying its morphology in detail; nevertheless, its extension can be roughly measured by fitting circular Gaussians to each image. The results of this procedure support the visual impression of a sharpening of the object with time: the FWHM of the best-fitting Gaussian changes from 0.33 ± 0.08 to 0.18 ± 0.02 arcsec in V_{606} and from 0.40 ± 0.10 to 0.19 ± 0.02 arcsec in I_{814}, while the value expected for point sources is about 0.15 arcsec.

3 THE LIGHT CURVE

Among the objects that could show variability at this high galactic latitude and faint flux level, active galactic nuclei (AGNs) and SNe are the most plausible candidates. The shape of the detected time variation and the possible development of a bright core in an underlying galaxy strongly suggest the identification of 2-584.2 with an SN observed soon after its explosion.

The expected evolution of the apparent magnitude of an SN can

[1] Images of 2-584.2 can also be found at http://www.arcetri.astro.it/~filippo/sn/sn.html and its brightening in V_{606} and I_{814}.

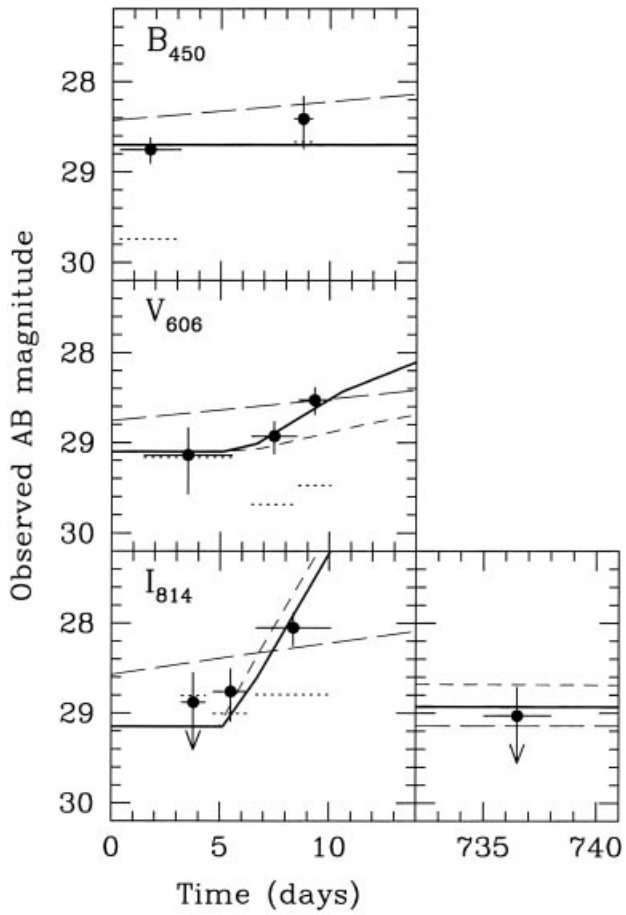

Figure 1. Photometry of 2-584.2 in B_{450}, V_{606} and I_{814} as a function of the (observer) time; day = 0 corresponds to the first observation. Each point shows the 1σ photometric errors and the time span covered by the data; the dotted lines are the 3σ limits of each image. The arrows in the I_{814} panels show the 3σ upper limits. The solid thick lines denote a fit obtained from a *K*-corrected, time-dilated SN Ib light curve at $z = 0.95$ with $t_{max} = 34.0$, $E(B-V) = 0.04$ and $\Omega_0 = 0.1$. The spectrum and the time evolution of an SN Ib simultaneously fit the magnitudes of the variable object and its evolution in the three filters. The underlying galaxy has $B_{450} = 28.70$, $V_{606} = 29.10$ and $I_{814} = 29.15$. Also shown are the curves for an SN Ia at $z \simeq 1.3$ (short-dashed line) and an SN II at $z \simeq 1.1$ (long-dashed line) which do not provide an acceptable match.

be derived from template light curves, spectra and absolute magnitude (as discussed below) once its distance is known and *K*-corrections (owing to the narrowing of the filter passband in the rest frame of the source and the redshifting of the emitted photons from the source to the observer) are computed. For high-redshift objects the time in the observer frame, t_{obs}, is related to the time in the supernova rest frame by $t_{obs} = (1+z)t_{rest}$; this produces a time dilation of the high-redshift SN light curve.

Once the SN template is given, four parameters are left to fit the data simultaneously in the various filters: the SN redshift, z, the time of maximum light, t_{max}, the colour excess owing to dust, $E(B-V)$, and the cosmological matter density parameter, Ω_0 (we assume $\Lambda = 0$). Some uncertainty remains associated with this fit, as pre-maximum light curves and spectra (particularly in the ultraviolet) are generally not very well determined because they are available only for a handful of objects. The SN flux must then be added to the host galaxy flux in each filter. The observed time variation of 2-584.2 shows that the SN quickly becomes dominant in V_{606} and I_{814} while the galaxy produces most of the B_{450} flux.

We now consider in turn the possibility that the detected variable source is a Type Ia (SN Ia), a Type II (SN II) or a Type Ib (SN Ib) supernova. SNe Ia have been shown to be reliable standard candles, as their intrinsic luminosities can be accurately determined (Phillips 1993). Pre-maximum optical (Cerro Tololo Interamerican Observatory, CTIO) and ultraviolet (*International Ultraviolet Explorer*, *IUE*) spectra of SN 1990N (Leibundgut et al. 1991) show that the flux drops off sharply below 2600 Å; therefore, as soon as $z \gtrsim 0.7$, their B_{450} flux is negligible as the cut-off is redshifted into this band, while the mere detection of variation in the V_{606} band puts the upper limit $z \gtrsim 1.6$. The luminosity of an SN Ia evolves in time according to a light curve (Leibundgut 1988; Doggett & Branch 1985) which shows a fast rise to the maximum (3.6 mag in 15 d), with slight differences between the (rest frame) *B* and *V* bands. When fitting the data for 2-584.2 with the time-dilated, *K*-corrected light curves, we find it impossible simultaneously to match the V_{606} and I_{814} data points (in this case the B_{450} data only give information on the galaxy magnitude), as shown in Fig. 1. Since the object is relatively faint, this implies high SN Ia redshifts ($z \gtrsim 1.3$) for which colours cannot be reproduced by using appropriate *K*-corrections. We conclude that identification of 2-584.2 with an SN Ia can be safely ruled out.

We repeat the same procedure for SNe II. These objects cannot be used as standard candles, as their peak abolute luminosities are known to cover a wide range, from $M_B \sim -14$ to ~ -19 (Patat et al. 1994). SNe II are usually divided into two classes (Doggett & Branch 1985): one (SN II-P) showing a slow pre-maximum brightening and a plateau in the after-maximum decline; the other (SN II-L) a faster brightening and a linear decline. In both cases the pre-maximum spectra can be approximated by a blackbody with a temperature $T_{BB} \sim 25\,000$ K (Kirshner 1990) without any UV cut-off. By comparing the expected light curves with the data (see Fig. 1), we can safely exclude both classes because (i) their brightening is too slow and (ii) their blue spectrum makes them too luminous in B_{450}.

SNe Ib yield a good agreement with the data. These objects closely resemble SNe Ia in terms of time evolution and spectra, but are typically 1–2 mag fainter (Wheeler & Levreault 1985; Kirshner 1990) and show a larger spread in the maximum brightness. While SNe Ia are found in all types of galaxies and derive from old stars, the SNe Ib are only detected near regions of active star formation and their progenitors should be young massive stars. As shown in Fig. 1, both the time evolution of 2-584.2 increasing from B_{450} to V_{606} to I_{814} and its apparent magnitudes are easily reproduced by SN Ib light curves (Kirshner 1990): acceptable fits can be obtained for $0.90 < z < 1.02$ which makes this object one of the most distant SNe observed to date, while the best agreement is found for $z = 0.95$, $t_{max} = 34.0 \pm 1$ d (∼12 rest-frame days after the end of the observations), low Ω_0 values and moderate reddening, $0 \leq E(B-V) \leq 0.05$ (Seaton 1979). This value of the reddening, corresponding to up to about 0.29 mag of extinction in V_{606} and 0.22 in I_{814}, could also be accounted for by an SN Ib fainter than the average and without extinction. Lower values for the fitting redshift tend to select low values of Ω_0 and low extinction, and vice versa for higher redshifts. The galaxy, showing flat $B_{450} - V_{606}$ and $V_{606} - I_{814}$ colours and luminosities indicating a star formation rate of about $0.2\,M_\odot\,yr^{-1}$ (Madau et al. 1998), is consistent with a star-forming dwarf. About 20 per cent of the flux in the I_{814} image taken two years later (*I*4) is still due to the SNe.

We therefore conclude that (i) SNe Ia are too bright and red and SNe II are too slow and blue to be viable candidates for 2-584.2, and (ii) an SN Ib naturally reproduces the time evolution,

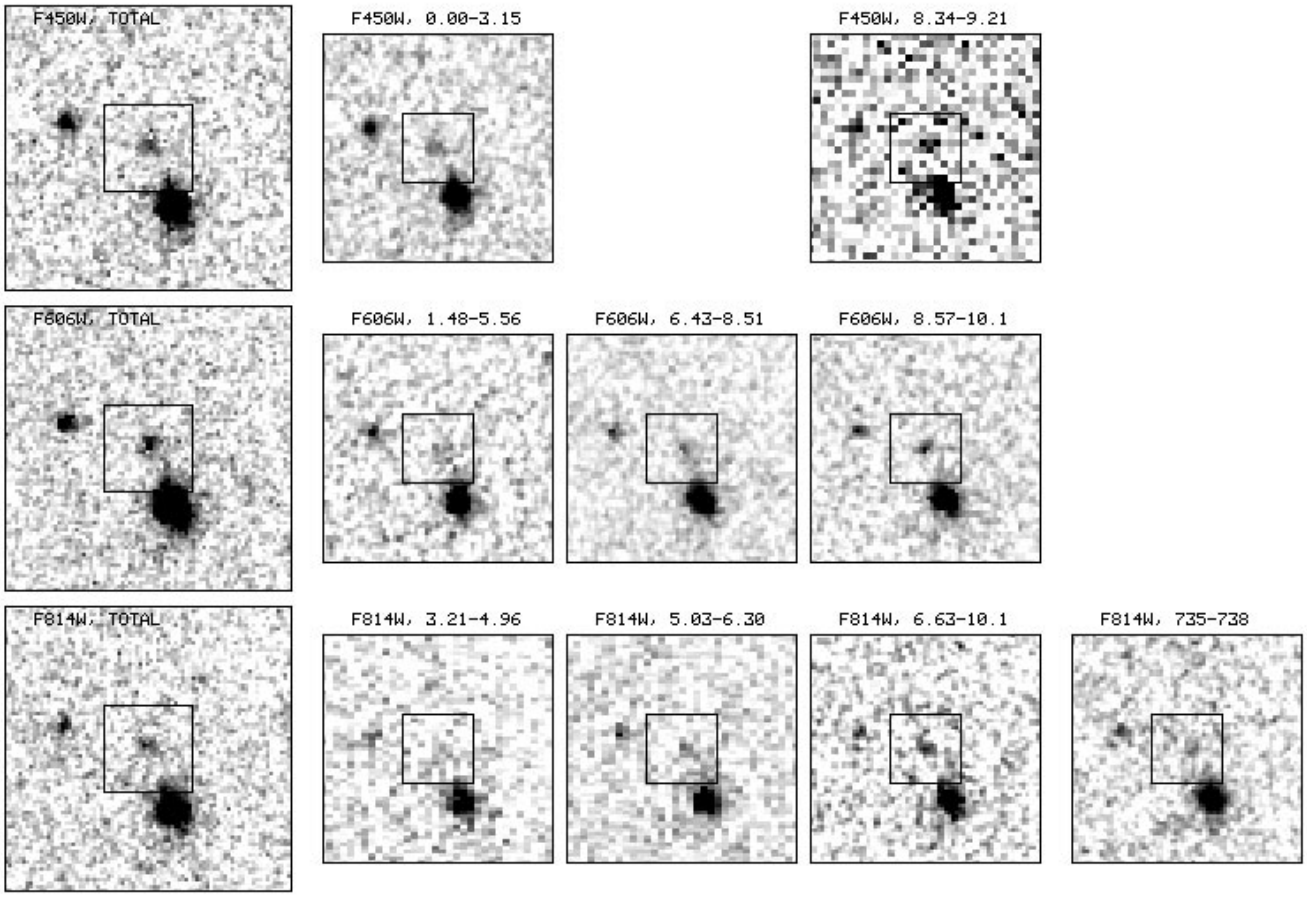

Figure 2. Images of 2-584.2 in the B_{450}, V_{606} and I_{814} bands. The three images on the left are the total HDF-N images by Williams et al. (1996)with a pixel scale of 0.04 arcsec pixel^{-1}. On the right the time sequence in each filter, with a pixel scale of 0.05 arcsec pixel^{-1}, shows the brightening of the object in V_{606} and I_{814} and its subsequent dimming. Each image is labelled by the filter and the time range of the observations in days. The size of the central squares is 1 arcsec.

brightness and colours of the variable object. This type of study, when applied to high-sensitivity future observations of long time span, could produce a significant sample of high-z SNe that could be successfully used to constrain the star formation history and the geometry of our Universe.

ACKNOWLEDGMENTS

We are indebted to P. Hoeflich and B. Leibundgut for providing supernova spectra and light curves, and to R. McCray, M. Salvati, L. Pozzetti and N. Panagia for useful discussions. We also thank the referee, R. Ellis, for insightful comments. We thank STScI/ST-ECF for the implementation of their data archive and for support during this work. FM acknowledges partial support from ASI grant ARS-98-116/22, AF acknowledges partial support as a Visiting Fellow at JILA.

REFERENCES

Aldering G., 1998, IAU Circ. 7046
Ciardi B., Ferrara A., 1997, ApJ, 483, L5
Couchman H. M. P., Rees M. J., 1986, MNRAS, 221, 53
Doggett J. D., Branch D., 1985, AJ, 90, 2303
Ferguson H. C., 1998, in Livio M., Fall S. M., Madau P., eds, The *Hubble Deep Field*. Cambridge Univ. Press, Cambridge, p. 181
Ferrara A., 1998, ApJ, 499, L17
Fruchter A. S., Hook R. N., Busko I. C., Mutchier M., 1997, in Casertano S., Jedrzejewski R., Keyes C. D., Stevens M., The 1997 *HST* Calibration Workshop with a New Generation of Instruments, Space Telescope Science Institute, Baltimore, p. 518
Garnavich P. et al., 1998, ApJ, 493, L53
Gilliland R. L., Phillips M. M., 1998, IAU Circ., 6810
Haiman Z., Rees M. J., Loeb A., 1997, ApJ, 484, 985
Kirshner R. P., Supernovae, Petschek A. G., 1990, Springer, New York
Leibundgut B., 1988, PhD thesis, University of Basel
Leibundgut B., Kirshner R. P., Filippenko A. V., Shields J. C., Foltz C. B., Phillips M. M., Sonneborn G., 1991, ApJ, 371, L23
Madau P., Della Valle M., Panagia N., 1998, MNRAS, 297, 17P
Madau P., Pozzetti L., Dickinson M., 1989, ApJ, 498, 106
Marri S., Ferrara A., 1998, ApJ, 509, 43
Marri S., Ferrara A., Pozzetti L., 1998, ApJ, submitted
Méndez R. A., Minniti D., De Marchi G., Baker A., Couch W. J., 1996, MNRAS, 283, 666
Miralda-Escudé J., Rees M. J., 1997, ApJ, 478, L57
Patat F., Barbon R., Cappellaro E., Turatto M., 1994, A&A, 282, 731
Perlmutter S. et al., 1998, Nat, 391, 51
Phillips M. M., 1993, ApJ, 413, L105
Sadat R., Blanchard A., Guiderdoni B., Silk J., 1998, A&A, 331, L69
Seaton M. J., 1979, MNRAS, 187, 73
Tegmark M., Silk J., Rees M. J., Blanchard A., Abel T., Palla F., 1997, ApJ, 474, 1
Thompson D., 1995, PhD thesis, Caltech
Valdes F., 1982, KPNO Internal Publication
Wheeler J. C., Levreault R., 1985, ApJ, 294, L17
Williams R. E. et al., 1996, AJ, 112, 1335

This paper has been typeset from a TEX/LATEX file prepared by the author.